Chapter 1

Introduction

In this chapter we have given a brief introduction to our current views of the basic building blocks of matter, deep inelastic scattering, structure functions, parton model, Regge theory and Quantum Chromodynamics and higher order corrections, various sum rules, non-perturbative QCD corrections such as nuclear effect, higher twist effect etc.

1.1   Our Current Views of Nature's Building Blocks

Particle physics is a quest for the fundamental building blocks of the matter, and the fundamental forces that operate to control and shape them. The pursuit for finding the "real" nature of the Universe is not only a means to satisfy instinctive curiosity but also a principal tool for the advancement and progress of civilization[1].

The search for the elementary constituents of nature has occupied generations of human beings since the speculations of the early Greek philosophers and other philosophers from different parts of the world. As far it is known, in the sixth century B.C. Thales proposed that all things reduced to water, and, coming out of the Greek-Roman eras and for centuries to come, the four basic elements were thought to be earth, water, fire, and air. Chinese (in Pinyin, Wu Xing) believed that these were earth, wood, metal, fire and water. Indians (Samkhya-Karika by Isvarakrsna) visualized the world as made of five elements: space, air, fire, water and earth. In about 400 B. C. the Greek philosophers Democritus and Leucippus proposed that matter is composed of indivisible particles called atoms, a word derived from a-(not)

and tomos (cut or divided)[2]. This idea lingered in the background for centuries until experimental support and through the work of eighteenth- and nineteenth-century chemists, brought atoms to the fore as the basic building blocks of matter.

The macroscopic quantities of homogeneous material can be divide or cut into parts such that each part retains the basic character of the original. But how far can such division be carried? If we cut a piece of gold into smaller and smaller snips, do we always get pieces of the gold? Is it possible that the divisions can go on forever, generating smaller and smaller snips of gold, or is there a limit such that no further divisions can be made or at least no further pieces leaving the parts as gold? If so what the final divisions consist of? Is there any constituent which is further indivisible?

From the earliest concepts to the resulting periodic table of elements, many small steps had been taken in our pursuit of the fundamental building blocks of nature and up to the end of nineteenth century the answer of this question was "atom". People believed that atoms are immutable and indivisible objects. By the close of the nineteenth century, however, the atoms were also under criticize and evolved the next question, "What are atoms made of?". Before discussing "What are atoms made of?", we would like to discuss something about elementary particles and how they are investigated.

The elementary particles are those particles which have no known structure, i.e., they are structure less or point like. They cannot be resolved into two or more parts. In order to investigate the possible structure of an object firstly we need to probe it by a probing beam which is scattered from the object. Analysing the diffraction pattern of scattered beam, we can remark on their structure. But whether a particle is point like or not it depends on the spatial resolution of the apparatus used. In case of an optical microscope, where the probing beam is light, the resolution is given by

$$\Delta r \simeq \frac{\lambda}{sin\theta} \tag{1.1}$$

where λ is the de Broglie wavelength of the incident beam of particles, which is given by $\lambda = \frac{h}{p}$. Here p is the beam momentum and θ is the angular aperture of the light beam used to view the structure of an object. For the improvement of resolution we need larger θ and smaller λ. Thus we see that the resolution depends on the initial momenta of the incident particle and to resolve an object we must have a probe whose wavelength is comparable or smaller than the size of the object. Again

from the uncertainty principle we have the relation, $\Delta p.\Delta x \geq \hbar c \approx 0.2 GeV fm$, which suggests that smaller the distance we want to probe, the beam energy must be higher. This is the underlying idea that is used to study the structure of particles and depending on the energy of the probing beam, the concept of elementary particle has been changing.

To resolve an atom we must have a probe whose wavelength is comparable or smaller than the size of the atom. The requirement of such type of probe was fulfilled by the alpha particle (ionized Helium atoms), which was the result of discovery of radioactivity of the substances in 1886 through the work of French physicist Henri Becquerel. It was observed that the alpha particles can be deflected in magnetic fields and therefore one could expect them to serve as natural weapons to study the atomic structure, in particular its charge distribution. Rutherford utilized this opportunity to investigate the basic structure of atoms. In 1911, he performed an experiment where a beam of alpha particles of a few MeV was fired into a thin sheet of gold foil. He observed that most of the alpha particles passed through the gold completely undisturbed, but a few of them bounced off at wild angles. Based on these observations Rutherford concluded that the positive charge, and virtually all of the mass of the atom was concentrated at the center occupying only a tiny fraction of the volume of the atom[3]. Furthermore, Rutherford was able to show by explicit calculation that the angular distribution of the scattered a particles agreed with that expected if they indeed interacted with a massive scattering center of positive charge Ze and which is in support his intuitive picture of the atom. The nucleus of the lightest atom (hydrogen) was given the name proton by Rutherford and thus the proton was inferred and later it was isolated in the laboratory. However before this, J. J. Thomson demonstrated the existence of a tiny particle which is much smaller in mass than hydrogen, the lightest atom. This was the electron, the first elementary particle which was discovered by Thomson in 1897[4]. In 1932 James Chadwick discovered the other constituent of nucleus, the neutron[5].

The dimension of the atom is typically $\sim 1\mathring{A} = 10^{-10} m \gg 10^{-15} m$, the dimension of proton. So the low energetic α particles could only resolved the atom and observed that an atom is made of a hard compact nucleus consisting of proton and neutron surrounded by a cloud of electrons. Due to the poor resolution, the proton and the neutron were regarded as point like or elementary particles. Up to 1950, the electron, proton and neutron were considered as the elementary particles.

By the early 1960s, accelerators reached higher energies, $\Delta E \gg 1 GeV$, which is required to probe proton. A parallel sequence of events occurred with the proton and neutron. In the 1960s very high energy electron beams were utilized at the Stanford Linear Accelerator Center (SLAC)[6] in an experiment that was analogous to the old alpha particle one in which the atomic structure was revealed. The electron beam was fired at protons and it was observed that the beam of electrons suffered violent collisions when it met the nucleons. The observation of these violent collisions suggested that the proton's charges were concentrated on some discrete scattering centres within, which in turn indicates the evidence of substructure of the proton. Comparison of the data on electron scattering with the analogous probing by neutrino beams has enabled us to learn about the nature, or quantum numbers, of the constituents of the proton. As a result of the above experiments, we have learned that the proton and neutron are therefore not elementary, but are made instead of the pointlike "quarks". The quarks are referred as point like because they have no internal structure or, more probably, that we have not yet resolved any constituent that they may have.

We observe that to Rutherford the nucleus appeared pointlike; more powerful beams of electrons reveal the inner structure of the nuclei and progressively resolved the neutrons and protons and finally using higher energy beams or equivalently shorter wavelength probes the substructure of the proton was uncovered. The use of high-energy particles showed that as the energies of the probing beam of the particles were increased, even smaller particles were obtained, which indicates the possibility of uncovering the substructure of quarks with further higher energetic beams. The quest, "What are the building blocks of nature?" has progressed from everyday objects to molecules, molecules to atoms, atoms to electrons and nuclei, nuclei to protons and neutrons, and protons and neutrons to quarks. Whether this progression to smaller and smaller components go on forever, or there will be the end with a single fundamental particle, that will be reflected in future particle physics research.

The birth of modern experimental particle physics in which particles were used to probe the structure of composite objects began with the famous alpha particle scattering experiment of Rutherford. The experimental effort originated by the end of the 19th century and the beginning of the 20th century with physicists, like Thompson, Rutherford, Chadwick and so on, discovering the presence of subatomic particles like electrons, nucleus etc. The use of high-energy particles as probe showed that as the energies of the colliding particles were increased, even smaller particles were obtained.

This led to the subsequent discovery of many particles like mesons, baryons, antiparticles, neutrinos etc. From the world of these particles, which are the outcome of many years of international effort through experiments, theoretical ideas and discussions, physicists have developed a theory called "The Standard Model" that explains the current understanding of elementary particle physics. The standard model is a simple, comprehensive, beautiful as well as the most successful theory in nature. The beauty of the Standard Model is twofold. On one hand it establishes the identity of all the elementary constituents of matter and on the other hand describes the fundamental forces that operate to control and shape matter. In accord with this model all the known matter particles are composites of quarks and leptons, held together by fundamental forces which are represented by the exchange of particles known as gauge bosons. The standard model is summarised in Table 1.1

J	Name	Symbol	Observed
0	Higgs Scalar	H	Yes
$\frac{1}{2}$	Leptons	$e,\ \mu,\ \tau,\ \nu_e,\ \nu_\mu,\ \nu_\tau$	Yes
	Quarks	$u,\ d,\ c,\ s,\ t,\ b$	Yes
	Photon	γ	Yes
1	Vector Mesons	$W^+,\ W^-,\ Z^0$	Yes
	Gluons	g	Yes
2	Graviton	G	No

Table 1.1: Particles in the Standard Model.

1.2   Deep Inelastic Scattering

Deep Inelastic Scattering(DIS)(cf. e.g. [7]) experiments have had an enormous impact towards the understanding of the fundamental constituents of matter. DIS provides one of the cleanest possibilities to probe the space-like short distance structure of nucleon through the interactions

$$l^\pm + N \longrightarrow l^\pm + X, \tag{1.2}$$

$$\nu_l(\bar{\nu}_l) + N \longrightarrow l^\pm + X, \tag{1.3}$$

and

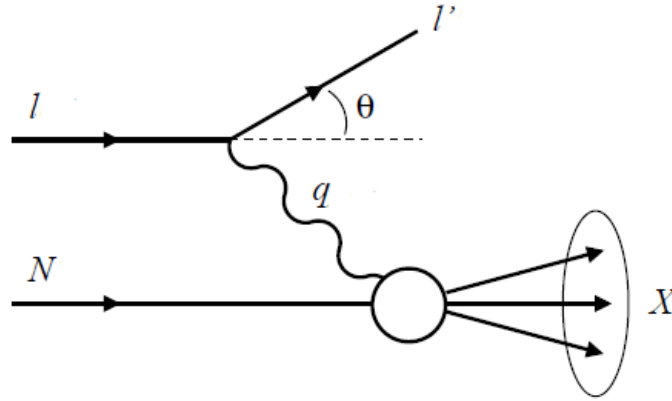$$l^\mp + N \longrightarrow \nu_l(\bar{\nu}_l) + X. \tag{1.4}$$

Figure 1.1: Schematic representation of deep inelastic scattering.

In DIS a charged lepton($l = e, \mu$), or a neutrino ($\nu_l = \nu_{e,\mu,\tau}$) is scattered off the nucleon(N) and produces a lepton and a shower of hadrons(X) in the final state. In this regard as the high energetic particles(lepton) probe deep within the target(nucleon), and as the target is disrupted after scattering, it is known as deep inelastic scattering. Various deep inelastic charged and neutral current interactions provide complementary sensitivity to reveal the quark flavor and gluonic structure of the nucleon. Moreover, polarized lepton scattering off polarized targets helps in the investigation of the spin structure of the nucleons.

1.2.1   Kinematics and Variables in DIS

The DIS processes at Born level can be illustrated as shown in Fig. 1.1. Here a lepton with momentum l scatters off a nucleon of mass M and momentum P via the exchange of a virtual vector boson (photon or Z_0 or $W^\pm$) with four momentum q. The four momenta of the outgoing lepton and the hadronic final states are l' and P_F respectively. The virtual boson has space like momentum with a virtuality Q^2, defined by

$$Q^2 \equiv -q^2, \tag{1.5}$$

where the four momentum transferred q is

$$q = l - l' = P_F - P. \tag{1.6}$$

In addition to Q^2 and q^2, other two important Lorentz invariant kinematic variables that describe the interaction are

$$s \equiv (P + l)^2 \tag{1.7}$$

and

$$W^2 = (P + q)^2 = P_F^2, \tag{1.8}$$

where s is the total center of mass energy squared and W represents the invariant mass of the hadronic final state. Further, in order to describe the scattering process, the Bjorken scaling variable x, the inelasticity y, and the total total energy transfer ν of the lepton to the nucleon in the nucleon's rest frame are usually referred and they are defined by

$$\nu \equiv \frac{P.q}{M}, \tag{1.9}$$

$$x \equiv \frac{-q^2}{2P.q} = \frac{Q^2}{2M\nu}, \tag{1.10}$$

$$y \equiv \frac{P.q}{P.l} = \frac{2M\nu}{s - M^2}. \tag{1.11}$$

1.2.2   Deep Inelastic Scattering Differential Cross Sections

Case 1: Charged Lepton DIS

The deep inelastic scattering differential cross section can be written in terms of products of two tensors, the leptonic tensor $L_{\alpha\beta}$ and the hadronic tensor $W_{\alpha\beta}$:

$$\frac{d^2\sigma}{dE'd\Omega'} \propto L_{\alpha\beta}W^{\alpha\beta}. \tag{1.12}$$

The leptonic tensor describes the lepton-photon interaction. Denoting the spin projections of the initial and final lepton by s and s' and then summing over s' the lepton tensor can be expressed in terms of two pieces which are symmetric and antisymmetric with respect to the Lorentz indices α and β:

$$L_{\alpha\beta} = L_{\alpha\beta}^s + iL_{\alpha\beta}^A, \tag{1.13}$$

where $L_{\alpha\beta}^s(k, k') = 2(k_\alpha k'_\beta + k_\beta k'_\alpha) + g_{\alpha,\beta}q^2$ and $L_{\alpha\beta}^A = 2m\epsilon_{\alpha\beta\mu\nu}s^\mu q^\beta$, with the lepton spin vector defined by $2ms^\mu = \bar{u}\gamma^\mu\gamma_5 u$. For unpolarized lepton scattering the average

over the initial lepton polarizations is performed and hence only the symmetric term, $L_{\alpha\beta}^s$, remains.

The hadronic tensor, $W^{\alpha\beta}$ provides complete information about the target response. The hadronic tensor can split into symmetric and antisymmetric parts:

$$W_{\alpha\beta} = W_{\alpha\beta}^s + W_{\alpha\beta}^A. \tag{1.14}$$

Lorentz and gauge invariance and symmetry properties together with parity conservation of the electromagnetic interaction imply the most general forms of these terms:

$$W_{\alpha\beta}^s = W_1(\nu, Q^2)\left(\frac{q_\alpha q_\beta}{q^2} - g_{\alpha\beta}\right) + \frac{W_2(\nu, Q^2)}{M^2}\left(P_\alpha - \frac{P.q}{q^2}q_\alpha\right)\left(P_\beta - \frac{P.q}{q^2}q_\beta\right) \tag{1.15}$$

and

$$W_{\alpha\beta}^A = i\epsilon_{\alpha\beta\mu\nu}q^\alpha\left[G_1(\nu, Q^2)S^\nu + \frac{G_2(\nu, Q^2)}{M^2}(S^\nu P.q - P^\nu S.q)\right]. \tag{1.16}$$

This defines four response functions $W_1(\nu, Q^2)$, $W_2(\nu, Q^2)$, $G_1(\nu, Q^2)$ and $G_2(\nu, Q^2)$. The first two can be measured in the unpolarized scattering, while the latter two require scattering of polarized leptons on polarized nucleons for their determination.

In the description of deep inelastic scattering process the response functions $W_{1,2}(\nu, Q^2)$ and $G_{1,2}(\nu, Q^2)$ are often replaced by the dimensionless structure functions $F_{1,2}(x, Q^2)$ and $g_{1,2}(x, Q^2)$, expressed in terms of the Bjorken variable x together with Q^2:

$$F_1(x, Q^2) = MW_1(\nu, Q^2), \tag{1.17}$$

$$F_2(x, Q^2) = \nu W_2(\nu, Q^2), \tag{1.18}$$

and

$$G_1(x, Q^2) = M\nu G_1(\nu, Q^2), \tag{1.19}$$

$$G_2(x, Q^2) = \nu^2\nu G_2(\nu, Q^2). \tag{1.20}$$

In terms of these structure functions, the unpolarized and polarized differential cross sections can be written as(with spin denoted by ⇑⇓)

$$\frac{d^2\sigma}{dxdy} = \frac{2\pi\alpha^2}{MEx^2y^2}\left[\left(1 - y - \frac{Mxy}{2E}\right)F_2 + xy^2F_1\right] \tag{1.21}$$

and

$$\frac{d^2\sigma \uparrow\Downarrow}{dxdy} - \frac{d^2\sigma \uparrow\Uparrow}{dxdy} = \frac{4\alpha^2}{MExy}\left[\left(2 - y - \frac{Mxy}{E}\right)G_1 - \frac{2Mx}{E}G_2\right] \tag{1.22}$$

respectively.

Case 2: Neutrino DIS

Like charged lepton DIS, neutrino-nucleon($\nu - N$) DIS experiments provide a good opportunity to study the structure of nucleon. The advantage of ν-DIS measurements over charged lepton experiments is that $\nu - N$ experiments can measure the structure function xF_3, in addition to F_1 and F_2. In the neutrino nucleon scattering, neutrino interacts weakly with the nucleon and due to parity violation in their weak interaction the third structure function xF_3 originates and the resultant differential cross section is given by

$$\frac{d^2\sigma^{\nu(\bar{\nu})}}{dxdy} = \frac{G_F^2 ME_\nu}{\pi(1 + Q^2/M_W^2)^2}\left[y^2 xF_1 + \left(1 - y - \frac{M_N xy}{2E_\nu}\right)F_2 \pm (y - \frac{y^2}{2})xF_3\right], \tag{1.23}$$

Where G_F is the Fermi weak coupling constant and M_W is the mass of the W boson mediating the interaction. Here $+(-)$ sign corresponds to the neutrino(antineutrino) scattering cross-section.

1.2.3   Bjorken Scaling

If the nucleon has substructure and that are resolvable for Q, $\nu \gg M$, then these W terms would be functions of the kinematic variables ν and Q^2:

$$W_1 \longrightarrow W_1(Q^2, \nu), \quad where \quad 2MW_1(Q^2, \nu) = \frac{Q^2}{2M\nu}\delta(1 - \frac{Q^2}{2M\nu}), \tag{1.24}$$

$$W_2 \longrightarrow W_2(Q^2, \nu), \quad where \quad \nu W_2(Q^2, \nu) = \delta(1 - \frac{Q^2}{2M\nu}), \tag{1.25}$$

$$W_3 \longrightarrow W_3(Q^2, \nu), \quad where \quad \nu W_3(Q^2, \nu) = \delta(1 - \frac{Q^2}{2M\nu}). \tag{1.26}$$

On the basis of analysis of various sum rules, Bjorken predicted that in the deep inelastic regime, where $Q^2 \rightarrow \infty$ and $\nu \rightarrow \infty$, the structure functions do not depend individually on (ν, Q^2) but only on their ratio $x = \frac{Q^2}{2M\nu}$. The variable x was first introduced by Bjorken and this feature is known as "Bjorken scaling"[8]. Soon after this prediction, approximate scaling behavior was observed experimentally in electron-proton scattering at SLAC[6]. The fact that the structure functions become independent of Q^2 indicates that the objects inside the nucleon from which one is scattering have no spatially extended structure, that is, one is scattering from point like constituents, known as "partons", about which we have discussed in the section 1.3.1. The scaling behavior of the structure functions are expressed as

$$MW_1 \longrightarrow F_1(x), \tag{1.27}$$

$$\nu W_2 \longrightarrow F_2(x), \tag{1.28}$$

and

$$\nu W_3 \longrightarrow F_3(x). \tag{1.29}$$

A similar scaling behavior is expected for the spin-dependent structure functions

$$g_1(x, Q^2) = M^2 \nu G_1(\nu, Q^2), \tag{1.30}$$

and

$$g_2(x, Q^2) = M \nu^2 G_2(\nu, Q^2), \tag{1.31}$$

which likewise reduce to functions of x only when the limit $Q^2 \rightarrow \infty$ is taken.

However, in the later experiments a small Q^2 dependence of the structure functions was also observed and this phenomena is known as scaling violation. Scaling violation is an important observable of QCD and discussed in the section 1.4.

1.3   Theoretical Models for the DIS Structure Functions

The first electron-proton scattering experiment was carried out at SLAC[6]. Immediately after these experiments several models were proposed to explain the behaviour

of the structure functions. The most prominent among them are Light Cone Expansion[9], Quark Parton Model(QPM)[10], Vector Meson Dominance Model(VMD)[11], Regge Pole Model[12, 13] and Dual Resonance Models[14]. Here we have provided a brief introduction to Quark Parton Model and Regge theory.

1.3.1   Quark Parton Model

In the early measurements, nucleon structure function in DIS, a weak dependence of structure functions on Q^2 was revealed, which in turn led to the conclusion that the virtual photon sees point-like constituents in the nucleon. In order to describe the composite nature of nucleons, the quark-parton model[10] was developed. In accord with quark-parton model, the nucleon is composed of free pointlike constituents, the partons, identified later as quarks and gluons. The basis of parton model is the introduction of parton distribution functions, $q_i(x)$ and $\bar{q}_i(x)$ for quarks and anti-quarks respectively, where $q_i(x)dx(\bar{q}_i(x)dx)$ signifies the probability of finding a quark(anti-quark) of flavor i in a nucleon, which carries a fraction x to $x + dx$ of the parent hadron's four-momentum p. Here x is the fractional four-momentum of the parent nucleon carried by a parton. On the basis of these ideas we can have a simple interpretation of nucleon structure functions F_1 and F_2 measured in charged lepton DIS as

$$F_1(x) = \frac{1}{2} \sum_{i=u,d,\dots} e_i^2 [q_i(x) + \bar{q}_i(x)], \tag{1.32}$$

and

$$F_2(x) = \frac{1}{2} \sum_{i=u,d,\dots} e_i^2 x [q_i(x) + \bar{q}_i(x)]. \tag{1.33}$$

They are thus related by the Callan-Gross relation[15],

$$F_2(x) = 2x F_1(x). \tag{1.34}$$

The Callan-Gross relation connecting F_1 and F_2 reflects the spin- $\frac{1}{2}$ nature of the quarks.

   The interpretation of structure functions measured in neutrino-DIS in accord with parton model is

$$F_2^{\nu(\bar{\nu})}(x) = \sum_{i=u,d,...} x[q_i^{\nu(\bar{\nu})}(x) + \bar{q}_i^{\nu(\bar{\nu})}(x)] \tag{1.35}$$

$$xF_3^{\nu(\bar{\nu})}(x) = \sum_{i=u,d,...} x[q_i^{\nu(\bar{\nu})}(x) - \bar{q}_i^{\nu(\bar{\nu})}(x)] \tag{1.36}$$

In the the naive parton model the spin-dependent structure functions g_1 and g_2 are given by

$$g_1(x) = \frac{1}{2} \sum_{i=u,d,...} e_i^2 \Delta q_i(x) \tag{1.37}$$

and

$$g_2(x) = 0. \tag{1.38}$$

where

$$\Delta q_i(x) = q_i^{\uparrow}(x) - q_i^{\downarrow}(x) + \bar{q}_i^{\uparrow}(x) - \bar{q}_i^{\downarrow}(x). \tag{1.39}$$

Here the helicity distributions $\Delta q_i(x) = q_i^{\uparrow}(x) - q_i^{\downarrow}(x)$ and $\Delta \bar{q}_i(x) = \bar{q}_i^{\uparrow}(x) - \bar{q}_i^{\downarrow}(x)$ involve the differences of the quark or antiquark distributions with helicities parallel and antiparallel with respect to the helicity of the target nucleon. The interpretation of $g_1(x)$ structure function can be understood from the fact that a virtual photon with spin projection $+1$ can only be absorbed by a quark with spin projection $-\frac{1}{2}$, and vice versa. In parton model, however the trasverse spin structure function g_2 vanishes identically and has been the subject of much theoretical debate [16].

1.3.2   Regge Theory

The study of scattering of hadronic particles, in the days before QCD was established, was based on Regge theory [12, 13]. The pre-QCD method, Regge theory relied basically on assumptions on the scattering matrix, such as Lorentz invariance, crossing symmetry, unitarity, causality, analyticity, asymptotic states etc., which determines the asymptotic behaviour of cross sections in the high energy limit regardless the strength of the coupling, i.e., independently of perturbation theory.

In accord with Regge theory the scattering amplitude for a two body scattering of hadrons ($2 \longrightarrow 2$ process) (Fig. 1.2) is given by the functional form[13]
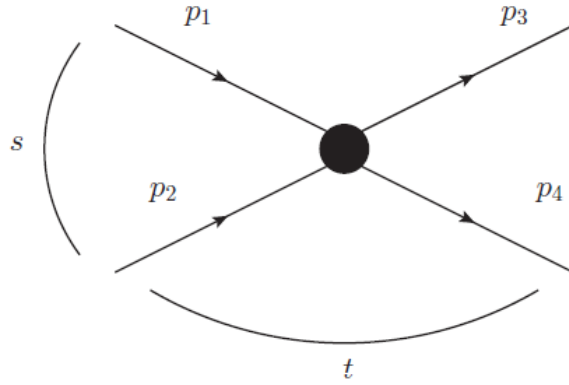
Figure 1.2: A $(2 \longrightarrow 2)$ scattering process.

$$A(s,t) \approx s^{\alpha(t)}. \tag{1.40}$$

for asymptotically large s, such as $s \gg t$. Here s is the center of mass energy, $t = (p_1 p_3)^2$, the momentum transfer and $\alpha(t)$ is a function of the momentum transfer t. Fig. 1.3 represents a typical diagram for the amplitude in Regge theory of the form Eq.(1.40).

The interactions in Regge theory that gives rise to an amplitude of the form Eq.(1.40) is successfully described by the exchange of a quasi-particle called Reggeon. Reggeons, like elementary particles, are characterized by quantum numbers such as charge, spin, etc. The spin of the Reggeons is a function of the momentum transfer t, and more specifically their spin is the function $\alpha(t)$ which appears in the equation for the amplitude Eq.(1.40).
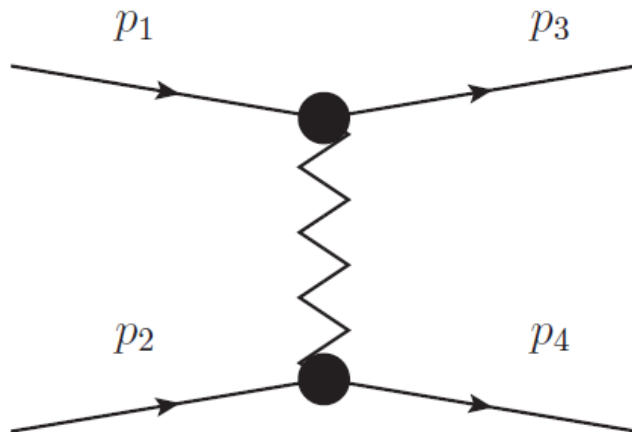

Figure 1.3: An interaction of two particles via the exchange of a Reggeon.

Although Reggeons are not real particles, but there are resonances at (half) integer spins and correspond to real particles of mass m and spin j, where $j = \alpha(m^2)$. By

plotting the square of the masses of various particles versus their spin, as shown in Fig. 1.4, it is observed that they lie along straight lines. These lines are the Regge trajectories

$$\alpha(t) = \alpha(0) + \alpha' t, \tag{1.41}$$

which correspond to the various quasi-particles in Regge theory. Here the intercept of the trajectory is $\alpha(0)$ and α' is the slope.
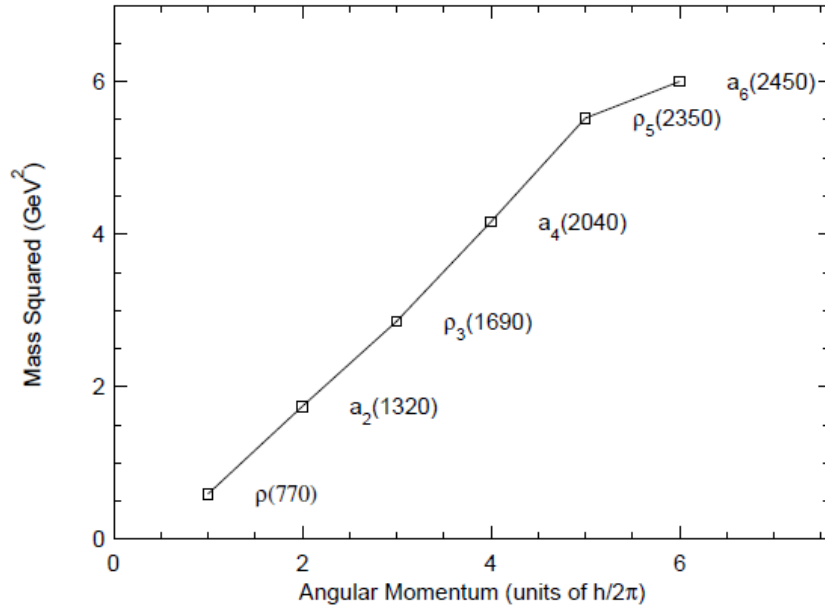

Figure 1.4: Plot of particle mass squared (in GeV^2) versus spin (in units of $\hbar$). It can be seen that the particles plotted lie along a linear trajectory, data taken from [17].

By utilising the Regge trajectories, asymptotic s dependence of the differential cross section can be obtained as

$$\frac{d\sigma}{dt} \propto s^{2(\alpha(0)+\alpha' t - 1)}, \tag{1.42}$$

where the singularity in $\alpha(t)$ with the largest real part, known as the leading singularity, determines the asymptotic behaviour of the scattering amplitude. The scattering amplitude helps in determining the total cross section and in the large s regime, where $s \gg t$, the behaviour of the total cross section is given by

$$\sigma_{tot} \propto s^{\sigma(0)-1}. \tag{1.43}$$

It is observed that the requirement for the growth of cross section is $\alpha(0) > 1$, i.e., the intercept has to be greater than one. However, the exchange which leads

to this growth in cross section can not be from a charged exchange as this would cause the cross section to vanish asymptotically. Instead the exchange requires to have the quantum numbers of the vacuum: no charge, no isospin, and a parity of $+1$. The experimental results on proton-proton scattering signifies a significant growth of the total cross section and this behaviour can be well explained by an exchange of a Reggeon with the trajectory [18]

$$\alpha(t) = 1.08 + (0.25 GeV^2)t. \tag{1.44}$$

Such an exchange which satisfies this trajectory is known as the Pomeron. More specifically this is referred to as the "soft" Pomeron to differentiate it from a "hard" Pomeron. No particle resonances have been observed on the Pomeron trajectory, however a particle that may lie along this path is proposed to be the glueball [19].

Although these models were seemed to be legitimate as far the early data are concerned, but their predictions show significant deviation from the recent measurements. With the advent of dedicated experimental facilities, now it is possible to determine the structure functions as well as different sum rules over a wide range of x and Q^2 with far greater precision than before. Recent experimental results are well described by Quantum Chromodynamics(QCD) and it is believed that QCD is a correct theory of strong interaction.

1.4   Quantum Chromodynamics

The Quantum Chromodynamics(QCD)(cf. e.g., [7, 20, 21]) is a theory of strong interaction – interactions between hadrons and, in particular, between their inner constituents. The Quark Parton Model(QPM) is based on the idea that DIS scattering cross sections may be determined from free quarks which are bound within the nucleon which is an apparent contradiction. Although QPM was very successful at being able to take parton distribution functions(PDFs) from one scattering process and predicting cross sections for other scattering experiments; it has several difficulties. Firstly QPM fails to describe accurately the violations of scaling and scale dependence of DIS cross sections. The fact that partons are strongly bound into colourless states is an experimental fact, but why they behave as free particles when probed at high momenta is inexplicable in QPM. The QPM is also unable to account for the total momentum of the proton via measurements of the momentum sum rule indicating the existence

of gluon. It is only by including the effects of the gluon and gluon radiation in hard scattering processes that an accurate description of experimental data can be given. These developments led to the formulation of Quantum Chromodynamics(QCD).

The successes of QCD in describing the strong interactions are summarized by two terms: asymptotic freedom and confinement. Asymptotic freedom refers to the weakness of the short distance interaction, while the confinement of quarks follows from its strength at long distance. It is an extraordinary feature of QCD that it accommodates both kinds of behaviour. Asymptotic freedom states that, as the distance between two quarks diminishes so does the effective strength of their interaction; and the particles become asymptotically free. On the other hand, as the distance between quarks increases, so does the effective interaction strength. Asymptotic freedom explains the absence of observed free quarks.

In perturbative QCD(pQCD), calculations are performed by expanding terms in a perturbation series in the coupling strength α_s. This is only valid when α_s is small, i.e., at high Q^2 (see Figs.1.5 and 1.6). The calculation of a scattering cross section in pQCD reduces to summing over the amplitudes of all possible intermediate states. Each graph is a symbolic representation for a term in the perturbative calculation. Leading Order(LO) term corresponds to the quark parton model and is considered to be of order α_s^0 in the perturbative expansion. LO Feynman diagrams have no gluon vertices as shown in Fig. 1.5. Next-to-Leading Order (NLO) diagrams add quark-gluon interactions to this pictures. NLO graphs have one gluon vertex and correspond to terms of order α_s^1 in the perturbative expansion. NLO Feynman diagrams for hard scattering are illustrated in Fig. 1.6. Similarly higher order terms such as NNLO, NNNLO etc., would correspond to addition of more gluon vertices two, three etc).

The four-momentum is conserved at each vertex. However, including higher order diagrams, the momentum circulating in the loop is not constrained. The integration over all momentum space for a loop diagram leads to logarithmic divergences when momentum goes to infinity. These type of divergences are treated in a systematic way by the renormalization technique. However the renormalization procedure introduces an arbitrary parameter μ, which has the dimension of mass.

Any physical observable F must be independent of the choice for μ, therefore we impose the following condition:

$$\mu^2 \frac{\partial F}{\partial \mu^2} = \left(\mu^2 \frac{\partial}{\partial \mu^2} + \mu^2 \frac{\partial \alpha_s}{\partial \mu^2} \frac{\partial}{\partial \alpha_s} \right) = 0. \qquad (1.45)$$
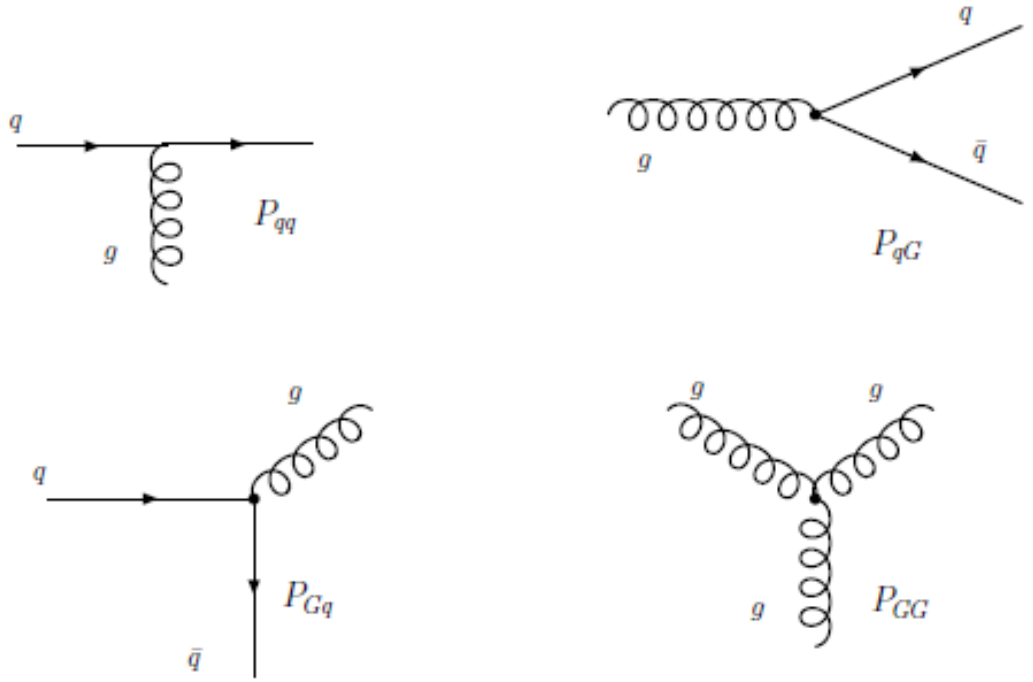
Figure 1.5: Leading Order splitting functions diagrams.

Hence, any explicit dependence of the physical observable on the renormalization scale must be cancelled by a proper renormalization scale dependence of α_s. The strong coupling α_s is determined by renormalization group equation given by

$$Q^2 \frac{\partial \alpha_s}{\partial Q^2} = \beta(\alpha_s) = -\frac{\beta_0}{4\pi}\alpha_s^2(Q^2) - \frac{\beta_1}{16\pi^2}\alpha_s^3(Q^2) - \frac{\beta_2}{64\pi^3}\alpha_s^4(Q^2) + O(\alpha_s^5), \qquad (1.46)$$

where the coefficients β_0, β_1 and β_2 depends on the number of active quark flavors n_f and scale Q^2 as

$$\beta_0 = 11 - \frac{2}{3}n_f, \qquad (1.47)$$

$$\beta_1 = 102 - \frac{38}{3}n_f, \qquad (1.48)$$

and

$$\beta_2 = \frac{2857}{6} - \frac{6673}{18}n_f + \frac{325}{54}n_f^2. \qquad (1.49)$$

Expansion of the β-function is carried out to three loops, which corresponds to a NNLO analysis.
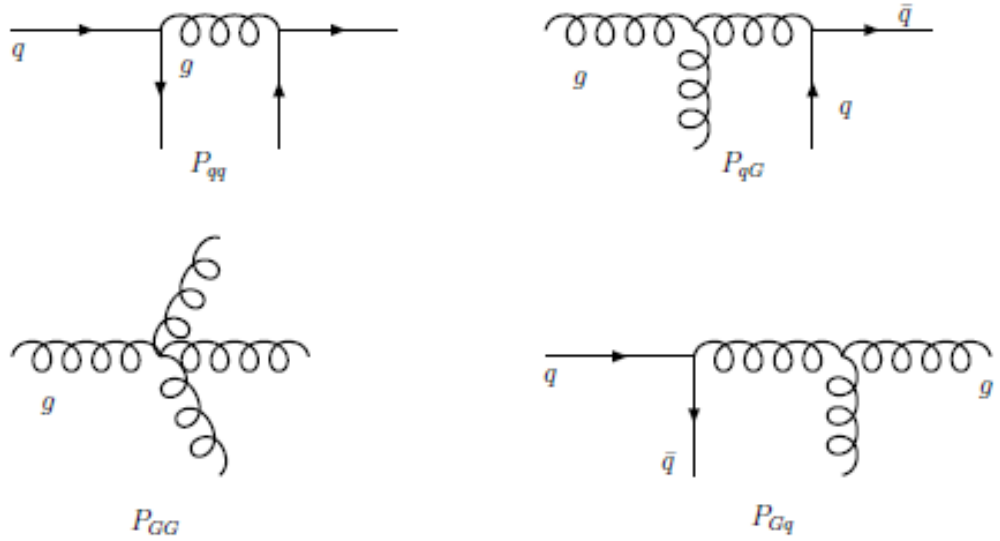
Figure 1.6: Examples of next-to-leading Order splitting functions diagrams.

The solution to renormalization group Eq.(1.46) provides the scale dependence of the strong coupling α_s, i.e. the "running" of α_s. Perturbative QCD predicts the scale dependence of the strong coupling, but α_s at a specific scale is obtained from experiment. Therefore, α_s at a reference scale is a fundamental parameter of the theory of QCD. Measuring the strong coupling from various experiments at different characteristic energy scales is an important test of QCD.

Moreover, one can introduce a dimensional parameter, Λ_{QCD},[22] to provide a parametrization of the scale dependence of the strong coupling α_s. In accordance with the convention of Ref.[22], $\Lambda_Q CD$ is defined by writing the solution of the renormalization group equation at LO, NLO and NNLO as[23]:

$$\left(\frac{\alpha(t)}{2\pi}\right)_{LO} = \frac{2}{\beta_0 t}, \tag{1.50}$$

$$\left(\frac{\alpha(t)}{2\pi}\right)_{NLO} = \frac{2}{\beta_0 t}\left[1 - \frac{\beta_1 \ln t}{\beta_0^2 t}\right], \tag{1.51}$$

$$\left(\frac{\alpha(t)}{2\pi}\right)_{NNLO} = \frac{2}{\beta_0 t}\left[1 - \frac{\beta_1 \ln t}{\beta_0^2 t} + \frac{1}{\beta_0^2 t^2}\left[\left(\frac{\beta_1}{\beta_0}\right)^2 (\ln^2 t - \ln t - 1) + \frac{\beta_2}{\beta_0}\right]\right],$$

where, $t = \frac{Q^2}{\Lambda_{QCD}^2}$ and Λ_{QCD} represents the scale at which perturbative QCD becomes strongly coupled, i.e. the scale for which the coupling α_s is large and perturbative QCD theory breaks down. The scale is comparable with the masses of the
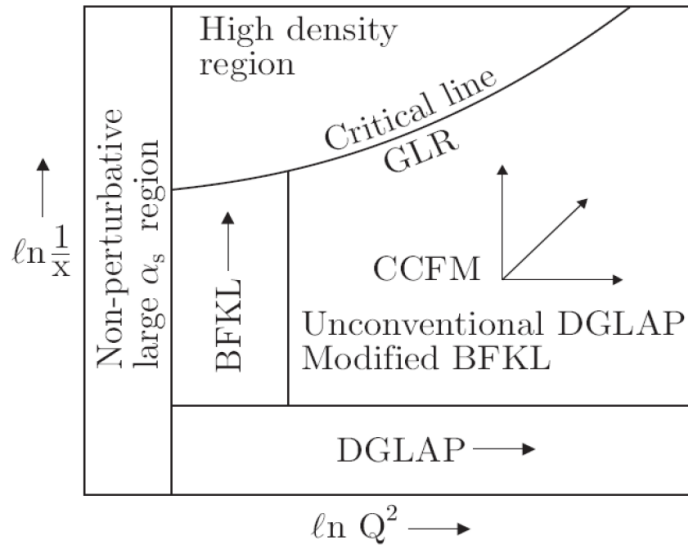
Figure 1.7: Schematic representation of the applicability of various QCD evolution equations across the $x - Q^2$ plane.

light hadrons($\approx 0.5 GeV$). In other words, Λ_{QCD} determines the boundary between quasi-free state of interacting quarks and gluons (weak coupling) and the state where hadrons are formed (strong coupling).

- **QCD Evolution Equations**

There exist several QCD evolution equations to obtain the quark and gluon distribution functions such as the Dokshitzer-Gribov-Lipatov-Alterelli-Parisi(DGLAP) equation[24], the Balitsky-Kuraev-Fadin-Lipatov(BKFL) equation[25], the Gribov-Levin-Ryskin(GLR) equation[26] and the Ciafaloni-Catani-Fiorani-Marchesini(CCFM) equation[27]. In spite of them, some other equations are also proposed like the Modified DGLAP equation (by Zhu and Ruan)[28], the Modified BKFL or BK[29] equation (by Balitsky and Kovchegov) and the JIMWLK[30] equation (by Jalilian-Marian, Iancu, McLerran, Weigert, Leonidov and Kovner) etc., in different kinematical regions. Schematic representation of the applicability of various QCD evolution equations across the $x - Q^2$ plane is depicted in Fig.1.7. Among these evolution equations, BFKL or GLR equations are more appealing at small-x, but still the DGLAP evolution equation is used to study various parton distrbution functions as well as the structure functions because this equation is a simple perturbative tool which is relevant for the presently accessible $x - Q^2$ range of structure functions.

Nucleon structure functions systematically exhibit a Q^2-dependence, even at large Q^2. These scaling violations can be described within the framework of the QCD-improved parton model which incorporates the interaction between quarks and gluons

in the nucleon in a perturbative way. The scale at which this interaction is resolved is determined by the momentum transfer. The Q^2-dependence of parton distributions, e.g.

$$F_2(x, Q^2) = \sum e_i^2 x [q_i(x, Q^2) + \bar{q}_i(x, Q^2)], \qquad (1.52)$$

$$xF_3(x, Q^2) = \sum x [q_i(x, Q^2) - \bar{q}_i(x, Q^2)] \qquad (1.53)$$

and

$$g_1(x, Q^2) = \frac{1}{2} \sum e_i^2 x [\Delta q_i(x, Q^2) + \Delta \bar{q}_i(x, Q^2)] \qquad (1.54)$$

are described by the DGLAP evolution equations. They are different for flavor non-singlet and singlet distribution functions. Typical examples of non-singlet combinations are the difference of quark and anti-quark distribution functions, or the difference of up and down quark distributions. The difference of the proton and neutron structure function, $F_2^p - F_2^n$, also behaves as a flavor non-singlet, whereas the deuteron structure function F_2^d is an almost pure flavor singlet combination. For the flavor non-singlet quark distribution, q^{NS}, and the flavor-singlet quark and gluon distributions, q^S and g, the DGLAP evolution equations read as follows[24]:

$$\frac{dq^{NS}(x, Q^2)}{d \ln Q^2} = \frac{\alpha(Q^2)}{2\pi} \int_x^1 \frac{dy}{y} q^{NS}(y, Q^2) P_{qq}(\frac{x}{y}), \qquad (1.55)$$

$$\frac{d}{d \ln Q^2} \begin{pmatrix} q^s(x, Q^2) \\ g(x, Q^2) \end{pmatrix} = \frac{\alpha(Q^2)}{2\pi} \int_x^1 \frac{dy}{y} \begin{pmatrix} P_{qq}(\frac{x}{y}) & P_{qg}(\frac{x}{y}) \\ P_{gq}(\frac{x}{y}) & P_{gg}(\frac{x}{y}) \end{pmatrix} \begin{pmatrix} q^s(y, Q^2) \\ g(y, Q^2) \end{pmatrix}. \qquad (1.56)$$

Here $\alpha(Q^2)$ is the running QCD coupling strength. The splitting functions $P_{ij}(x/y)$ are calculable in perturbative QCD as a power series of $\alpha_s(Q^2)$:

$$P_{ij}(z, \alpha_s(Q^2)) = P_{ij}^{(0)}(z) + \frac{\alpha_s}{2\pi} P_{ij}^{(1)}(z) + \left(\frac{\alpha_s}{2\pi}\right)^2 P_{ij}^{(2)}(z). \qquad (1.57)$$

Splitting functions are known up to NNLO[31,32]. The splitting functions $P_{ij}(\frac{x}{y})$ give the probability of parton j with momentum fraction y be resolved as parton i with momentum fraction $x < y$. They are calculated perturbatively to a given order in α_s. LO and NLO splitting function diagrams are shown in Figs. 1.5-1.6. Evolution equations describe the physical picture in which valence quarks are surrounded by a

cloud of virtual particles which are continuously emitted and absorbed. The quarks are also emitting and absorbing virtual particles of their own, corresponding to the branching probability densities. This picture explains why the structure of the hadron appears to change as it is seen at different distance scales. Thus, at low Q^2 there are fewer partons and their PDFs are skewed to high momentum fractions. At high Q^2, the momentum is shared through the parton branchings, and hence the low x region is filled with gluons and sea quarks which have a high probability to undergo $g \rightarrow gg$, $g \rightarrow q\bar{q}$ branchings. QCD doesn't predict the PDFs at any scale, rather it predicts how PDFs evolve with the scale through the evolution equations.

1.5   DIS Sum Rules

The structure functions which parameterize the deeply inelastic scattering cross section obey a series of sum rules to which QCD corrections are also available[7,33] and one may perform QCD tests using these relations. Sum rules are integrals over structure functions or parton distributions and they are associated with the conservation law for some quantum number of the nucleon. Parton model sum rules provide information about the distribution of quarks inside nucleon and are very useful to reveal new physics if a sum rule is found to be satisfied or broken. In the following subsections, we have discussed briefly about some important sum rules along with available pQCD corrections.

1.5.1   Gottfried Sum Rule

The Gottfried Sum Rule(GSR)[34,35] involves the difference of F_2 measured in proton and neutron targets using a charged lepton. In accord with parton model it is governed by

$$S_G = \int_0^1 \frac{F_2^{\mu p} - F_2^{\mu n}}{x} dx = \frac{1}{3}. \tag{1.58}$$

There are pQCD corrections to GSR up to 3-loop corrections[35] and it is given by

$$S_G = \int_0^1 \frac{F_2^{\mu p} - F_2^{\mu n}}{x} dx = \frac{1}{3}\left[1 + 0.0355\frac{\alpha_s}{\pi} - 0.811(\frac{\alpha_s}{\pi})^2\right]. \tag{1.59}$$

1.5.2 Adler Sum Rule

The Adler Sum Rule[36,37] predicts the integrated difference between neutrino-neutron and neutrino-proton structure functions. It states

$$S_A = \int_0^1 \frac{F_2^{\nu n} - F_2^{\nu p}}{2x} dx = 1. \tag{1.60}$$

The ASR is exact and receives neither QCD nor mass corrections, but its experimental verification is at a very low level of accuracy[37].

1.5.3 Gross-Llewellyn Smith Sum Rule

The Gross-Llewellyn Smith Sum Rule(GLSSR)[38,39] involves an integration over the non-singlet neutrino structure function, $xF_3(x, Q^2)$, which is obtained by subtracting the antineutrino differential cross section on an isoscalar target from the corresponding neutrino cross section. It is the most accurately tested sum rule. The GLSSR predicts that the number of valence quarks in a nucleon, up to finite Q^2 corrections, is three. In the QPM, the GLS sum rule reads[38]:

$$S_{GLS} = \int_0^1 \frac{xF_3}{x} dx = \frac{1}{3}, \tag{1.61}$$

and pQCD correction to GLS sum rule up to NNLO is given by[39]

$$S_{GLS}(Q^2) = \int_0^1 \frac{dx}{x} xF_3(x, Q^2) = 3\left[1 - \frac{\alpha_s}{\pi} - a(n_f)\left(\frac{\alpha_s}{\pi}\right)^2 - b(n_f)\left(\frac{\alpha_s}{\pi}\right)^3\right]. \tag{1.62}$$

1.5.4 Unpolarized Bjorken Sum Rule

The Unpolarized Bjorken Sum Rule(UBSR)[40] refers to the integrated difference between neutrino-neutron and neutrino-proton charged current structure functions F_1.

$$S_{Bj} = \int_0^1 \frac{F_1^{\nu n} - F_1^{\nu p}}{d} x = 1. \tag{1.63}$$

It has three loop pQCD correction, which predicts[41]

$$S_{Bj} = \int_0^1 \frac{F_1^{\nu n} - F_1^{\nu p}}{d} x = \left[1 - \frac{\alpha_s}{\pi} - a(n_f)\left(\frac{\alpha_s}{\pi}\right)^2 - b(n_f)\left(\frac{\alpha_s}{\pi}\right)^3\right]. \tag{1.64}$$

1.5.5   Polarized Bjorken Sum Rule

Polarised Bjorken Sum Rule(BSR)[42] relates the difference of proton and neutron structure functions integrated over all possible values of Bjorken variable, x to the nucleon axial charge g_A as

$$S_{BSR} = \int_0^1 \frac{dx}{x} x g_1^{NS}(x, Q^2) = \frac{g_A}{6}. \tag{1.65}$$

However, away from $Q^2 \to \infty$, the polarized BSR is given by a series in powers of the strong coupling constant $\alpha_s(Q^2)$[43]:

$$S_{BSR}(Q^2) = \int_0^1 \frac{dx}{x} x g_1^{NS}(x, Q^2) = \frac{g_A}{6} \left[1 - \frac{\alpha_s}{\pi} - 3.583 (\frac{\alpha_s}{\pi})^2 \right.$$
$$\left. -20.215 (\frac{\alpha_s}{\pi})^3 + ... \right]. \tag{1.66}$$

Here the BSR consists of pQCD results up to third order of $\alpha_s(Q^2)$. BSR is associated with the conservation of polarised isospin.

1.5.6   Gerasimov-Drell-Hearn Sum Rule

Gerasimov-Drell-Hearn Sum Rule(GDHSR)[44] is given by the first moment of the polarized structure function $g_1^{p,n}(x, Q^2$ in the form

$$S_{GDHSR}(Q^2) = 2\frac{M^2}{Q^2} \int_0^{x_0} dx g_1^{p,n}(x, Q^2) = \begin{cases} -\frac{1}{4}\mu_{p,n}^2, & Q^2 \to 0 \\ \frac{2M^2}{Q^2}\Gamma_1^{p,n}, & Q^2 \to 0 \end{cases}. \tag{1.67}$$

at proton and neutron targets, with $x_0 = Q^2/(2Mm_\pi + m_\pi^2 + Q^2)$, $\mu_{p,n}$ the anomalous magnetic moment of the proton or nucleon, and Γ_1 the first moment of the structure function g_1 at infinite space-like momentum transfer. This sum-rule has a very strong Q^2-evolution for low values of the virtuality. In case of proton targets it changes sign between $Q^2 = 0$ and $Q^2 \approx 1 GeV^2$.

In addition to these there are several important sum rules such as Burkhardt-Cottingham sum rule[45], Efremove-Teryaev-Leader sum rule[46], Ellis-Jaffe sum rule[47], etc., however in this thesis we have concentrated on GSR, GLSSR and BSR, which are associated with the non-singlet structure functions F_2^{NS}, xF_3 and g_1^{NS} respectively. The determination of these sum rules are provided in chapter 7.

1.6   Non-Perturbative QCD Effects

At low Q^2, the strong coupling constant becomes large and the perturbative calculations fail. In this non-perturbative region the assumption of scattering from massless, point-like, quarks is no longer valid. Also, the resolving power is not large enough to probe a single quark scattering. To obtain high interaction rates, lepton DIS experiments use heavy targets. Therefore, nuclear effects must be considered as well. These non-perturbative effects are discussed in the following subsections.

1.6.1   Target Mass Correction

At low Q^2 and high x, one can not neglect the effects of the target mass. The meaning of x as the fraction of the nucleons momentum carried by the struck quark is not suitable when $Q^2 \approx M^2$. A "target mass" correction must be applied to account for these effects. The target mass correction (TMC) to the structure functions have been first determined in [48]. More recently, new derivations were performed in [49] which lead to the following relations:

$$F_2^{TM}(x, Q^2) = \frac{x^2}{\xi^2} \frac{F_2^{(0)}(x, Q^2)}{k^3} + \frac{6M_p^2 x^3}{Q^2 k^4} \int_\xi^1 \frac{F_2^{(0)}(u, Q^2)}{u^2} du$$
$$+ \frac{12M_p^4 x^4}{Q^4 k^5} \int_\xi^1 du \int_u^1 \frac{F_2^{(0)}(v, Q^2)}{v^2} dv, \qquad (1.68)$$

$$F_3^{TM}(x, Q^2) = \frac{x}{\xi} \frac{F_3^{(0)}(x, Q^2)}{k^2} + \frac{2M_p^2 x^2}{Q^2 k^3} \int_\xi^1 \frac{F_3^{(0)}(u, Q^2)}{u} du \qquad (1.69)$$

with ξ and k are defined as

$$k = \sqrt{1 + \frac{4x^2 M_p^2}{Q^2}}, \qquad (1.70)$$

and

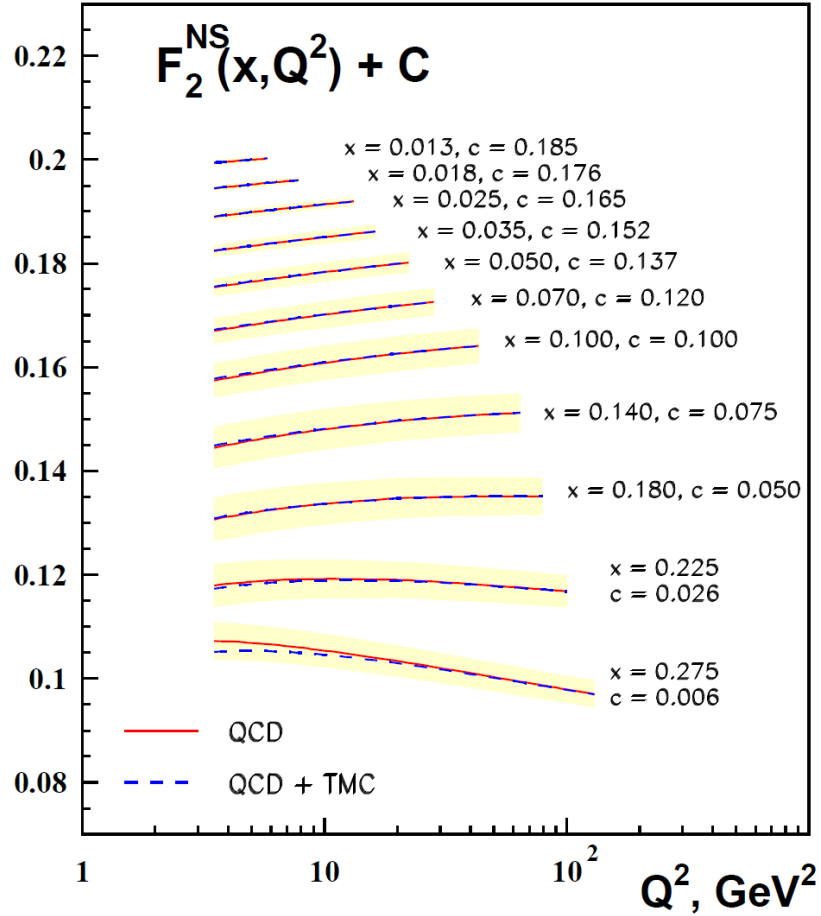$$\xi = \frac{2x}{1 + k} \qquad (1.71)$$

respectively.

Figure 1.8: The contribution from target mass corrections(TMC) to F_2^{NS} structure function. Figure is taken from[50].

The target mass effects are large at high x and low Q^2. Fig. 1.8 shows the size of the the TMC, as obtained in Ref. [50] for $F_2^{NS}(x, Q^2)$ structure functions along with QCD prediction as a function of x. As our kinematical region of consideration is within low-x and low-Q^2 region in our thesis we have neglected the effects of TMC.

1.6.2   Higher Twist

The Operator Product Expansion(OPE)[51] is a common theoretical framework in analyses of deep inelastic scattering(DIS) in QCD. The operators can be ordered according to their twist yielding the series in $\frac{1}{Q^2}$ for physical observable. For example, for the structure function F_i, this reads

$$F_i(x, Q^2) = F_i^{LT}(x, Q^2) + \frac{h_i(x)}{Q^2}. \tag{1.72}$$

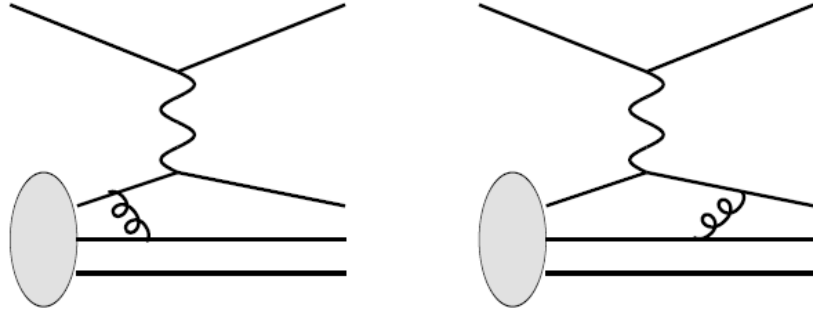The first term in this expansion (the leading twist, LT) dominates at sufficiently large

Figure 1.9: Examples of higher twist QCD diagrams.

momentum transfer Q^2 and invariant mass $W^2 = M^2 + \frac{Q^2(1-x)}{x}$. The LT structure functions are constructed in terms of parton distribution functions (PDFs), which are universal for charged lepton and neutrino scattering and have clear probabilistic interpretation. An accurate knowledge of these plays a key role in the extraction of possible contributions of new physics at new collider energies, non-accelerator physics (cosmic neutrinos) and, as observed more recently, in the interpretation of forthcoming high precision experiments on neutrino oscillation.

The higher-twist terms include interactions with other quarks, as shown in Fig. 1.9. Since target mass effects also involve powers of $\frac{1}{Q^2}$, they are referred to as "Kinematic higher-twist" effects. The scattering involving a conglomerate of quarks processes are referred to as "Dynamical higher-twist". These effects are important at low Q^2 and high x. The higher-twist contributions are calculated using phenomenological approaches. However, our analysis uses data in the kinematic range where these effects are negligible. Therefore, only kinematical higher-twist (not the dynamical higher twist) effects are studied.

1.7   Nuclear Effects

Although the primary aim of the DIS experiments is to explore the structure of nucleon, DIS data is collected usually for nuclear targets. The use of nuclei instead of nucleon serve a dual purpose in the studies of in high-energy scattering experiments. Firstly, nuclear DIS provides unique possibilities to study the space-time development of strongly interacting systems and it can provide valuable insights into the origin of nuclear force and properties of hadrons in nuclear medium. Secondly, the nuclear data often serve as the source of information on hadrons otherwise not directly accessible (e.g., extraction of the neutron structure function which is usually obtained from

deuterium and proton data). Moreover, in experiments with nucleon targets the products of the scattering processes can only be observed by a detector that is far away from the collision point, whereas a nuclear target can serve as a detector located at the place where the microscopic interaction takes place. Consequently, with nuclei one can study coherence effects in QCD which are not accessible in DIS off nucleons.

When considering DIS on a nuclear target one may expect that the resulting nuclear structure functions were very similar to those measured off a nucleon target. This is so because the nucleons are very loosely tighted inside a nucleus, and the interaction between the external probe, the virtual photon, and the constituent nucleons could be expected to be incoherent.

However, in 1982, the European Muon Collaboration(EMC)[52] reported that the ratio

$$R(x, Q^2) = \frac{F_2^A(x, Q^2)}{F_2^N(x, Q^2)}, \tag{1.73}$$

where F_2^A and F_2^N are the nuclear and nucleon structure functions respectively, is in general, different from one. The observed difference between the nuclear structure function and that corresponding to the simple addition of its constituent nucleons is commonly referred to as the EMC effect[53] and that was the first clear evidence for the nuclear effect in nuclear structure functions. In fact, the EMC effect states that, in the parton point of view, quark distributions in bound nucleon are different from those in free nucleon.

Whether there is enhancement or suppression of the nuclear structure functions with respect to those of the nucleon depends on the kinematical region of interest[53–55]. The general Bjorken-x dependence of such modification is as follows(see Fig. 1.10):

1. The ratio R is smaller than unity within the region $x < 0.01$. This region is known as **shadowing**.

2. Within $0.1 \leq x \leq 0.25 \sim 0.3$ the ratio R is larger than unity. This region is called **anti-shadowing**.

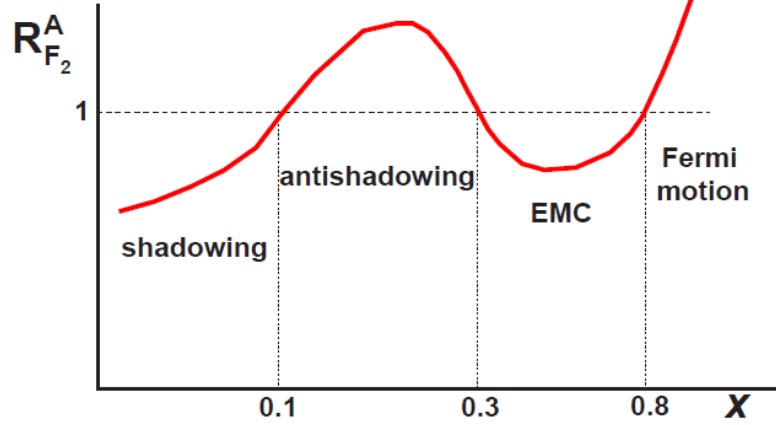3. Within $0.25 \sim 0.3 \leq x \leq 0.8$, R is smaller than unity and this region is known as the **EMC region**.

Figure 1.10: x dependence of the ratio $R^A_{F_2}(x, Q^2)$ for a given fixed Q^2.

4. $x \geq 0.8$, R is greater than unity and this region is known as **Fermi motion region**.

The nuclear effects are large at low and high x, but are observed to be independent of Q^2. However, there are new theoretical treatments that consider a Q^2 dependent nuclear target corrections at low x[57, 227]. Recent results from NuTeV hint that neutrino experiments might favor smaller nuclear effects than the charged lepton experiments[58] at high x, but this thesis does not take into account Q^2 dependent nuclear corrections. We can interpret our extracted PDFs from QCD fits as effective nuclear PDFs, which have the nuclear effects absorbed into them. These nuclear effects are discussed in detailed in chapter 8. □□